ON THE POSSIBILITY OF TIDAL FORMATION OF BINARY PLANETS AROUND ORDINARY STARS

Philipp Podsiadlowski[1], Saul Rappaport[2], John M. Fregeau[3,4], Rosemary A. Mardling[5]
Submitted to ApJ

ABSTRACT

The planet formation process and subsequent planet migration may lead to configurations resulting in strong dynamical interactions among the various planets. Well-studied possible outcomes include collisions between planets, scattering events that eject one or more of the planets, and a collision of one or more of the planets with the parent star. In this work we consider one other possibility that has seemingly been overlooked in the various scattering calculations presented in the literature: the tidal capture of two planets which leads to the formation of a binary planet (or binary brown dwarf) in orbit about the parent star. We carry out extensive numerical simulations of such dynamical and tidal interactions to explore the parameter space for the formation of such binary planets. We show that tidal formation of binary planets is possible for typical planet masses and distances from the host star. The detection (or lack thereof) of planet–planet binaries can thus be used to constrain the properties of planetary systems, including their mutual spacing during formation, and the fraction of close planets in very eccentric orbits which are believed to form by a closely related process.

Subject headings: accretion, accretion disks — planets and satellites: general — celestial mechanics — methods: *N*-body simulations — planets and satellites: formation — stars: binaries: eclipsing — stars: low-mass, brown dwarfs — stars: planetary systems: formation — stars: planetary systems: protoplanetary disks

1. INTRODUCTION

The Earth–Moon and the Charon–Pluto systems are sometimes referred to as double (or binary) planets, i.e., binary systems consisting of two planets whose center of mass orbits a central star. These rocky systems are likely to have formed by the fissioning of a more massive planet due to a giant impact (Hartmann & Davis 1975; Lin 1981; Canup & Asphaug 2001). In this study, we are interested in binaries of gas giant planets (or even brown dwarfs) for which a fission origin is unlikely. Specifically, we investigate whether such systems can form by tidal interactions and their implications for planet formation. The discovery of such systems in current or future searches for planet transits (such as the Kepler [Basri et al. 2005] and CoRoT missions [Auvergne et al. 2009]) is exciting for a number of reasons. These include (i) the fact that the existence of binary giant planets could provide strong observational evidence for tidal capture as a viable astrophysical mechanism. (ii) Binary planets would allow for new and important tests and models of planetary dynamics early in the formation process of planetary systems, including their mutual spacing during formation. (iii) They would also allow for studies of long-term planetary dynamics, including current measures of internal structure via apsidal motion, and spin-orbit interactions. (iv) Binary planets would provide un-

precedented accuracy for determining masses, radii, internal structure, etc. (v) It seems quite possible that an eclipsing set of planets, transiting a parent star, would provide more information on the oblateness of the planets than a simple transit light curve (see, e.g., Carter & Winn 2010), especially given that such a system would be expected to be rotating more rapidly than a single planet orbiting the parent star. (vi) Finally, if there is any significant amount of "magnetic braking" in a close binary planet system, the two planets could actually be driven into Roche lobe contact, leading to mass transfer between the planets. Such a planetary mass-transfer system would most likely be quite stable and very long lasting.

The formation of a binary planet is intimately linked to the evolution of the protoplanetary disk from which the planets have formed and within which they evolve. When the two planets are still embedded in a gaseous disk, they may migrate inwards or outwards, transferring orbital angular momentum to or from the disk. If the migration is relatively slow, the two planets may evolve into an isolated low-order mean-motion resonance and will then migrate together locked in this resonance (Lee & Peale 2002; Papaloizou & Szuszkiewicz 2005). Such a stable configuration precludes the formation of binary. However, if sufficient eccentricity is somehow induced during the migration process, or if the migration process is sufficiently fast to push the system through the resonance, neighboring resonances can destabilize the system. More generally, the orbits of two planets become dynamically unstable when the fractional difference of their orbital radii becomes sufficiently small (Gladman 1993). The presence of a disk can inhibit the development of an instability by limiting the growth of eccentricities. But once the stabilizing influence of the disk disappears, e.g., because of a decrease of the disk mass (more specifically, the disk

[1] University of Oxford, Department of Astrophysics, Keble Road, Oxford, OX1 3RH, UK; podsi@astro.ox.ac.uk
[2] M.I.T., Department of Physics and Kavli Institute for Astrophysics and Space Research, 70 Vassar St., Cambridge, MA 02139, USA; sar@mit.edu
[3] Kavli Institute for Theoretical Physics, UCSB, Santa Barbara, CA 93106, USA; fregeau@kitp.ucsb.edu
[4] Chandra/Einstein Fellow
[5] School of Mathematical Sciences, Monash University, Clayton, Victoria 3800, Australia; rosemary.mardling@sci.monash.edu.au

surface density) or because the planets have grown sufficiently by accretion from the disk, the planet orbits can become unstable. This will generally lead to a dynamical scattering event, in which the configuration of the planets can change drastically. Ford & Rasio (2008) and Chatterjee et al. (2008) have systematically studied such scattering events in systems with two and three planets and found that the results of such scatterings could be: (a) the collision and merger of the two planets, (b) the collision and merger of a planet and the host star, (c) the ejection of one of the planets, or (d) a quasi-stable configuration in which both planets remain orbiting the host star after $\sim 10^6$ orbits. However, these authors did not consider another possibility: the formation of a binary planet. The latter may result either from a three-body exchange or more simply from a tidal capture (Fabian et al. 1975).

A tidal capture occurs when the two planets get sufficiently close – typically within a few planet radii – but do not collide directly. Such close encounters induce tidal oscillations in one or both planets, converting orbital energy into oscillation energy (which is eventually dissipated as thermal energy) and leaving a bound binary planet (at least temporarily) in orbit about the host star. During subsequent periastron passages, energy may be exchanged either to or from the tides (unless the tidal oscillations have been completely damped in the mean time), and the evolution is formally chaotic (Mardling 1995) in much the same way as an unstable three-body orbit (again with the possibility of dissociation). During this phase, the tides can be extremely large (because the tidal amplitude is additive), and it is likely that nonlinear fluid processes such as shocks operate to make energy dissipation quite efficient, limiting the amplitude of the tides. However, once the system has dissipated a sufficient amount of tidal energy, it will cease to behave chaotically and will circularize in the normal fashion with the tidal amplitude never being able to grow (Mardling 1995). In the case that tidal capture occurs in the tidal field of a third body (in the present case, the star), the tidal energy exchange process can be *doubly* stochastic. However, to simplify the modeling process, we will assume in this work that all energy deposited in the tides is dissipated before the next periastron passage, consistent with severe tidal damping during this phase as discussed above. The validity of this assumption depends on the efficiency of the tidal dissipation process, often parametrized using the tidal Q value (e.g., Goldreich & Soter 1966).

In a three-body exchange, a binary planet forms by the "exchange" of the outer planet into the "inner binary" (the central star + inner planet) forming a new inner binary (the two planets). If there is no dissipation of orbital energy, the newly formed pair is susceptible to dissociation because, unlike a normal two-body tidal capture, it is continuously forced by the tidal field of the star. The binary orbit will exchange energy and angular momentum with its center-of-mass orbit around the star in a random-walk fashion (the system is formally chaotic; Mardling 2008), until sufficient energy has been transferred to the binary to dissociate it. This can only be avoided once enough orbital energy is *permanently* removed from the binary to make the system stable against chaotic interactions. This can occur through

(point-mass) interactions with other bodies (e.g., a third planet or a background of planetesimals), similar to the mechanism proposed for the formation of Kuiper-Belt binaries (Goldreich et al. 2002), or through tidal dissipation if the planets are close enough.

In both scenarios, tidal dissipation may play a key role in forming a binary planet, but, in the first case, the tidal capture has to operate in one (or possibly a few) encounters, while, in the second, tidal dissipation may operate over the much longer timescale of the transient binary state. We therefore expect that, in the first case, the post-capture orbital separation of the binary planet is a few planet radii, while, in the second, it could be as wide as is stable on a long time timescale.

In this study, we consider primarily the mutual tidal capture of two planets in a "dynamically active" planetary system. We show that, for reasonable assumptions about the tidal coupling and dissipation of gas giant planets, mutual tidal capture of planets into a planet–planet binary is a relatively generic feature of dynamically systems. In this regard, it has recently been shown that the long-standing issue of the relatively high eccentricities of extrasolar planets can be understood if the configuration of the newly-formed planetary system after the gas disk has dissipated is dynamically active, so that planet–planet scattering can operate and eject planets while increasing the eccentricities of the remaining planets (Ford & Rasio 2008; Jurić & Tremaine 2008; Chatterjee et al. 2008). It is not obvious that planetary systems forming via the usual core accretion scenario should result in dynamically active systems after the gas disk phase. However, simulations starting with protoplanets in a gas disk and following both gas physics and N-body dynamics have shown that such resulting configurations are indeed possible (Thommes et al. 2008; Matsumura et al. 2010).

Based on our calculations, we present the *relative* probabilities of the possible outcomes of dynamically active systems (including, e.g., planet–planet collisions, tidal capture, ejection). We discuss the potential observability of a planet binary in relation to the likelihood that planetary systems are dynamically active early in their lifetimes.

In our study we also allow for the possibility of tidal capture of *brown dwarfs* (BDs) in close orbit around a hydrogen-burning star. Brown dwarfs probably form in a very different way from, and at a different distance than, gas giant planets. While gas giants likely form via core accretion, any brown dwarf forming out of a circumstellar disk will do so via gravitational fragmentation, and at fairly large distances from the host star ($\gtrsim 10^2$ AU), where the disk is Toomre unstable (Toomre 1964) and can cool sufficiently so that unstable clumps can collapse (see, e.g., Stamatellos & Whitworth 2009; also see Boss 1997). We do not address the issue of how to get the brown dwarfs to distances of $\lesssim 1$ AU from the host star, but note that such systems are known to exist (e.g., CoRoT 15b contains a brown dwarf orbiting an F star with an orbital period of 3 d; Bouchy et al. 2010). In any case, as we will show, if multiple brown dwarfs exist on such close orbits, they can easily become bound in a BD–BD binary via tidal capture.[6]

---

[6] Throughout this paper, we do not sharply distinguish between planets and brown dwarfs and often refer to all types of sub-stellar

In §2 we present the results of numerical simulations of dynamically active planet systems for a range of masses and distances from the parent star. In §3 we describe the detectability of such binary planets in radial velocity searches and in transit studies.

2. NUMERICAL SIMULATIONS

2.1. *Numerical Method*

Since the dynamical processes leading to planet–planet tidal capture are the same as those that lead to planet–planet collisions, any numerical method which can properly treat "dynamically active" planetary systems should serve as an appropriate base upon which we can add a treatment of tidal dissipation. We use the *Fewbody* integrator, which is designed for strong small-N-body gravitational encounters (Fregeau et al. 2004). We have tested that the code is suitable for simulating dynamically active planetary systems by comparing our results to the simulations of Ford & Rasio (2008) (see Appendix).

In order to include tidal capture, we also had to include a treatment of tidal dissipation in *Fewbody*. We use the functional fits to the energy dissipated by the close passage of two polytropes as presented in Portegies Zwart & Meinen (1993). When the two planets, of mass m_i and radius R_i, encounter each other with close approach distance less than $10(R_1 + R_2)$, we calculate the energy dissipated in the encounter by treating each planet as an $n = 3/2$ polytrope and reduce the planet–planet relative velocity (at pericenter) accordingly. We only include tidal dissipation in impulsive interactions, requiring – somewhat arbitrarily – that the close approach distance is less than 10% of the previous local maximum in the planet–planet distance.[7] This provides a lower limit on the overall tidal dissipation. If the close approach distance is less than $R_1 + R_2$ we assume the planets merge instantaneously, conserving mass and momentum.

2.2. *Stability Criterion*

Fewbody automatically terminates a calculation when an unambiguous, dynamically stable configuration has been obtained. To accurately test for the dynamical stability of a binary planet orbiting a star, we use the newly improved algorithm of Mardling (2008), which utilizes the concept of orbital resonance overlap to test for chaos and, ultimately, instability. The resonance overlap algorithm in its current form is only approximate for small values of the outer eccentricity $e_{\rm out}$, i.e., the eccentricity of the outermost body (in this context the parent star) about the center of mass of the innermost binary (the planet-planet binary). We thus set $e_{\rm out} = 0.1$ in the algorithm when the outer eccentricity is smaller than this value. In addition, we also require that the apocenter of the planet–planet orbit is within 2/3 of its Hill radius at pericenter. Specifically, we require

$$a_{\rm in}(1 + e_{\rm in}) < \frac{2}{3} a_{\rm out}(1 - e_{\rm out}) \left(\frac{m_1 + m_2}{3M_\star} \right)^{1/3}, \quad (1)$$

objects collectively as planets.

[7] This means that no tidal damping is applied for eccentricity $\lesssim 0.8$ in a bound planet-planet system.
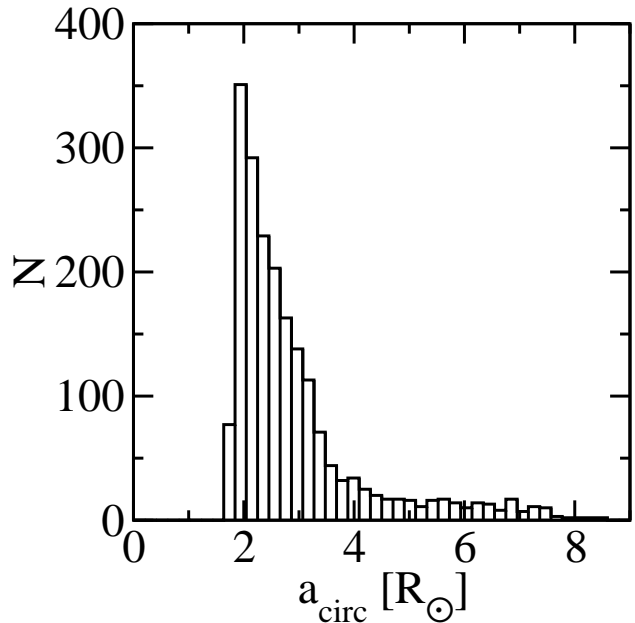

Fig. 1.— Histogram of semi-major axes of circularized binary brown dwarfs resulting from tidal capture events in model t21 (with brown dwarfs masses of $30\,M_{\rm J}$ and $70\,M_{\rm J}$, respectively).

where $a_{\rm in}$ and $e_{\rm in}$ are the semi-major axis and eccentricity of the newly formed planet–planet binary, and the expression on the right is 2/3 the radius of the Hill sphere of the planet–planet pair evaluated at apocenter.

2.3. *Starting Conditions*

We adopt initial conditions for our simulations that are similar to those of Ford & Rasio (2008). The planet masses are either $m_1 = 10^{-3}\,M_\odot$ and $m_2 = 0.5 \times 10^{-3}\,M_\odot$ for the "gas giant" case, or $m_1 = 70 \times 10^{-3}\,M_\odot$ and $m_2 = 30 \times 10^{-3}\,M_\odot$ for the "brown dwarf" case. In all cases, we fix the central star's mass at $M_\star = 1\,M_\odot$, and planet 1 initially orbits with semi-major axis $a_{1,\rm init} < a_{2,\rm init}$. We use three initial values for a_1: $a_{1,\rm init} = 0.2$, 1, and 5 AU. The initial semi-major axis of planet 2 is set so that the system is not Hill stable, with $a_{2,\rm init}$ randomly distributed uniformly between $0.9a_{1,\rm init}(1 + \Delta_c)$ and $a_{1,\rm init}(1 + \Delta_c)$, where $\Delta_c = 2.4(m_1/M_\star + m_2/M_\star)^{1/3}$ (Gladman 1993). The planet initial eccentricities $e_{i,\rm init}$ are randomly distributed uniformly between 0 and 0.05, and the relative inclination of the planet orbits is distributed uniformly between $0°$ and $2°$. All remaining orbital elements are sampled uniformly in their allowed range. For reference, all model parameters are shown in Table 1.

2.4. *Thermal Bloating of the Interacting Planets*

In this study, we assume that each of the pair of planets/brown dwarfs was born early in the evolutionary history of the parent star. In particular, we adopt the hypothesis that the planets/brown dwarfs were either born separately in the unstable collapse of a massive accretion disk, or otherwise were driven to migration toward the parent star via an accretion disk. In either case, the planets or brown dwarfs were necessarily young when they captured each other, i.e., had an age of $\sim 1 - 30$ Myr. Planets, and especially brown dwarfs, are quite
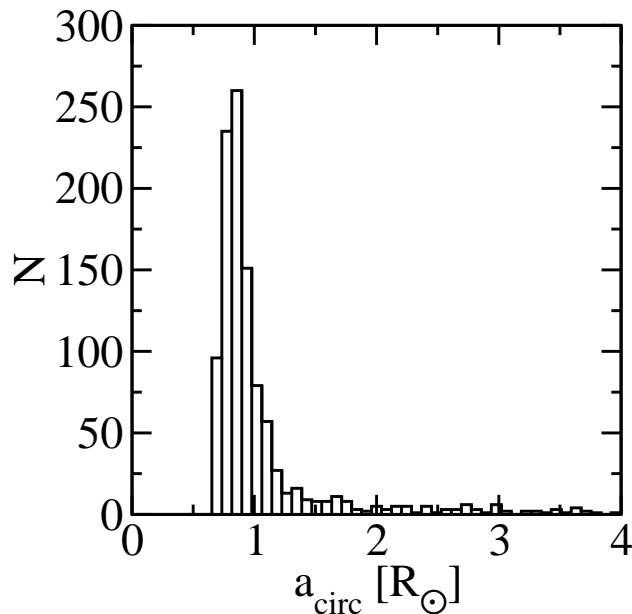
FIG. 2.— Histogram of semi-major axes of circularized binary planets resulting from tidal capture events in model t16 (with planet masses of $1\,M_{\rm J}$ and $0.5\,M_{\rm J}$, respectively).

thermally bloated at these young ages (see, e.g., Fig. 4 of Nelson et al. 1993). We have constructed a semi-empirical fitting formula for the radius of brown-dwarfs of mass $\gtrsim 15\,M_{\rm J}$ as a function of evolution time, t, as follows:

$$R(t) = 0.79\sqrt{M_i/M_{\rm J}}\,t_6^{-1/3}\,R_{\rm J}\,, \qquad (2)$$

where t_6 is the evolution time in units of 10^6 yr, M_i is the mass of the planet, and $M_{\rm J}$ and $R_{\rm J}$ are the mass and radius of Jupiter, respectively. This expression works quite well for masses above $\sim 20\,M_{\rm J}$ and for ages in the range of $0.1-30$ Myr. For any object whose radius falls below $1\,R_{\rm J}$ based on this expression, we simply fix the radius at $1\,R_{\rm J}$.[8]

Tidal dissipation is a strong function of the radius of the planet or brown dwarf compared to its separation from the object with which it is interacting. Hence, the inclusion of thermal bloating is potentially important, as it allows tidal capture to occur at larger initial separations.

After a planet–planet binary is formed via tidal capture and the resulting star–planet–planet system is deemed dynamically stable by the Mardling (2008) stability criterion, we stop the calculation and record the semi-major axis, $a_{\rm in}$, and eccentricity, $e_{\rm in}$, of the planet–planet binary. In post-processing we assume the orbit is quickly tidally circularized, and set $a_{\rm circ} = a_{\rm in}(1 - e_{\rm in}^2)$. Fig. 1 shows a histogram of the circularized planet–planet semi-major axes resulting from tidal capture events in model t21 (for a pair of brown dwarfs). There is a clear peak just above $a_{\rm circ} \approx 2\,R_\odot$, with a tail that extends out to $\sim 8\,R_\odot$. Fig. 2 shows the distribution for model t16 (for a pair of giant gas planets).

2.5. Illustrative Scattering Results

---

[8] Note that this prescription may underestimate the radii of very close Jupiter-mass planets that could be inflated due to tidal heating (Bodenheimer et al. 2001).
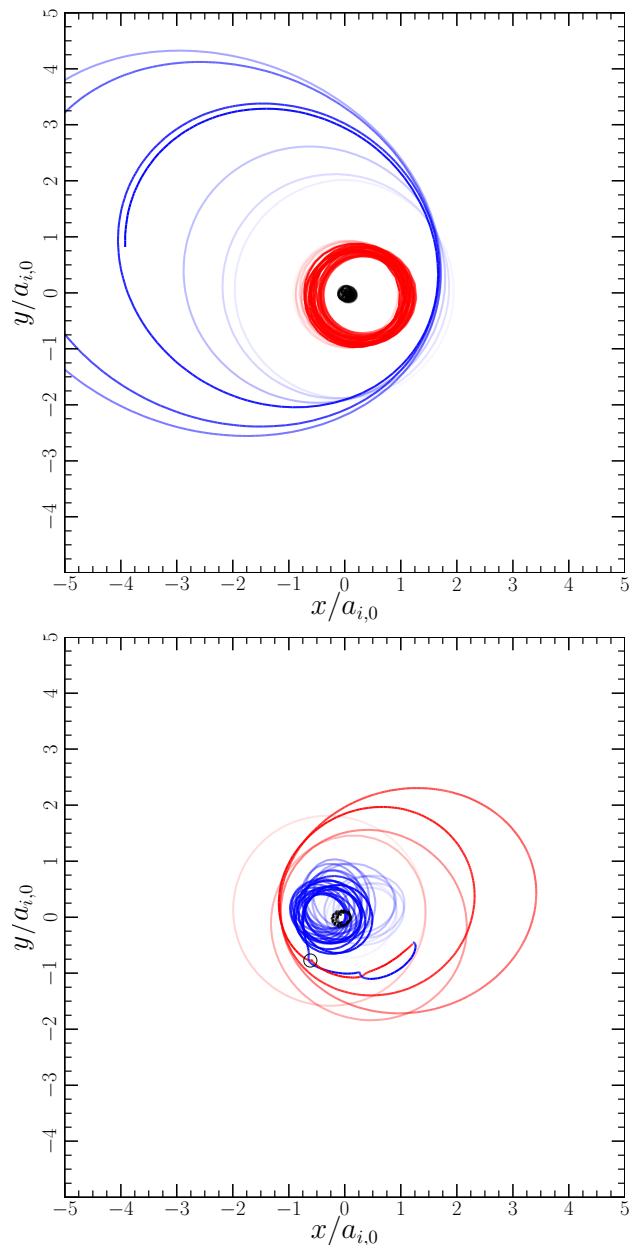

FIG. 3.— Evolution of a planet/brown dwarf binary system from model t21 in the x–y plane at the start of the calculation (upper panel), and at the end of the calculation (lower panel). The star is represented by a black trail, and the planets by red and blue trails. The trails fade with time so that the darkest points along a curve are the most recent. Dissipative tidal encounters are shown as open circles at the point where they occur. The system becomes active quickly after the start of the calculation. Over time the planets exchange position relative to the star. The planets suffer a weak dissipative tidal encounter at late time but eventually collide and merge.

To get a better feel for how the dynamics unfolds in a simulation resulting in tidal capture, we have plotted the evolution of the star and 'planet' positions for a set of representative simulations from model t21.[9] Fig. 3 shows a typical simulation ending in a *merger* of the two planets. The system becomes active quickly after the

---

[9] Model t21 is a simulation for brown dwarfs, but the scattering results for the planet simulations are very similar.
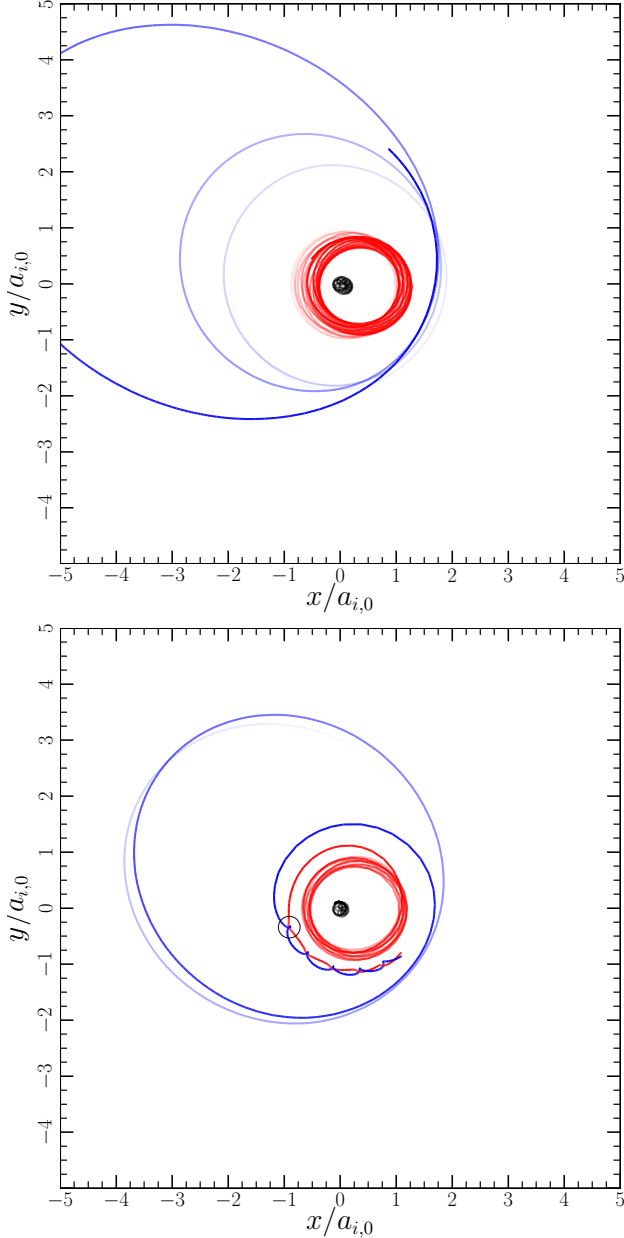
FIG. 4.— Evolution of a planet/brown dwarf binary system from model t21 resulting in tidal capture. Conventions are as in Fig. 3. The system becomes dynamically active shortly after the calculation begins. A strong tidal encounter at a later time binds the planet–planet pair, resulting in a configuration that is dynamically stable. The planet–planet binary's circularized semi-major axis is $2.3\,R_\odot$.

start of the calculation. Over time the planets exchange position relative to the star. The planets suffer a weak dissipative tidal encounter at late time but eventually collide and merge.

Fig. 4 shows a typical *"direct" tidal capture* simulation. The system becomes dynamically active shortly after the calculation begins. A strong tidal encounter at a later time binds the planet–planet pair, resulting in a configuration that is dynamically stable. The planet–planet binary's circularized semi-major axis is $2.3\,R_\odot$. Fig. 5, on the other hand, shows a typical *"gradual" tidal capture* simulation. A weak tidal encounter (the smaller

of the two open circles) nearly results in a dynamically stable planet–planet binary. The planets later suffer a stronger tidal encounter (the larger of the two open circles) that results in a stable configuration. In this case, the planet–planet binary's circularized semi-major axis is $6.0\,R_\odot$. These "gradual" tidal captures are responsible for the long tails in the final semi-major axis distributions in Figs. 1 and 2.

2.6. *Summary of Scattering Results*

For reference, we give the outcome statistics for each model in Table 2. We also show in Fig. 6 a summary of the fraction of dynamically active systems in which one of the planets is ejected as a function of the different assumed distances from the parent star, and in Fig. 7 the fraction of systems leading to a successful tidal capture.

2.7. *Simulated Population of Binary Planets*

Based on the results of the numerous scattering events that we have computed for a wide range of masses and distances from the parent star, we have devised a simple fitting formula that approximates the distribution for forming a tidally-captured binary pair of planets or brown dwarfs with a (final) circularized orbital separation, $a_{\rm circ}$. Expressed in Monte Carlo form, we have:

$$a_{\rm circ}(X) = \left(\frac{R_{i,\rm bloat}}{R_{\rm J}} \right) \left(\frac{1}{3} + \frac{0.1X}{1-X} \right) \; R_\odot \,, \quad (3)$$

where $R_{i,\rm bloat}$ is the thermally bloated radius of the larger of the planets/brown dwarfs at the time of tidal capture, $R_{\rm J}$ is the radius of Jupiter, and X is a uniformly distributed random number between 0 and 0.99 (the upper limit in X introduces an upper cutoff of $a_{\rm circ} \simeq 10\,R_\odot$, above which our scattering experiments provide insufficient statistics). While the overall probabilities for tidal capture do vary systematically with distance from the parent star (see Table 2) and the masses of the scattering objects, the basic functional form of the distribution of $a_{\rm circ}$, and its dependence on the radii of the tidal capturing planets, seem relatively independent of distance and masses.

Once we have in place analytic expressions for the thermal bloating as a function of age, and the distribution of tidal-capture circularized orbital radii as a function of the thermal bloating, we can use these to generate a synthetic population of binary planets and brown dwarfs. In this simulation, we first choose a random location, d, for the planet/brown dwarf binary between 0.01 and 10 AU, uniformly distributed in $\log d$. This is completely arbitrary since we do not know *a priori* the initial distribution of where planets and brown dwarfs form in a protoplanetary disk. Next, we choose a random age for the planet/brown dwarf pair between 1 and 15 Myr, uniformly distributed in $\log t$. The age sets the size of the thermally bloated radius according to equation (2). The final (late-age) circularized orbital separation, $a_{\rm circ}$, of the binary is chosen randomly from the distribution given by equation (3). Finally, we choose the eccentricity of the outer orbit (i.e., the orbit of the CM of the planet/brown-dwarf binary around the parent star) from the following probability distribution derived from our scattering studies:

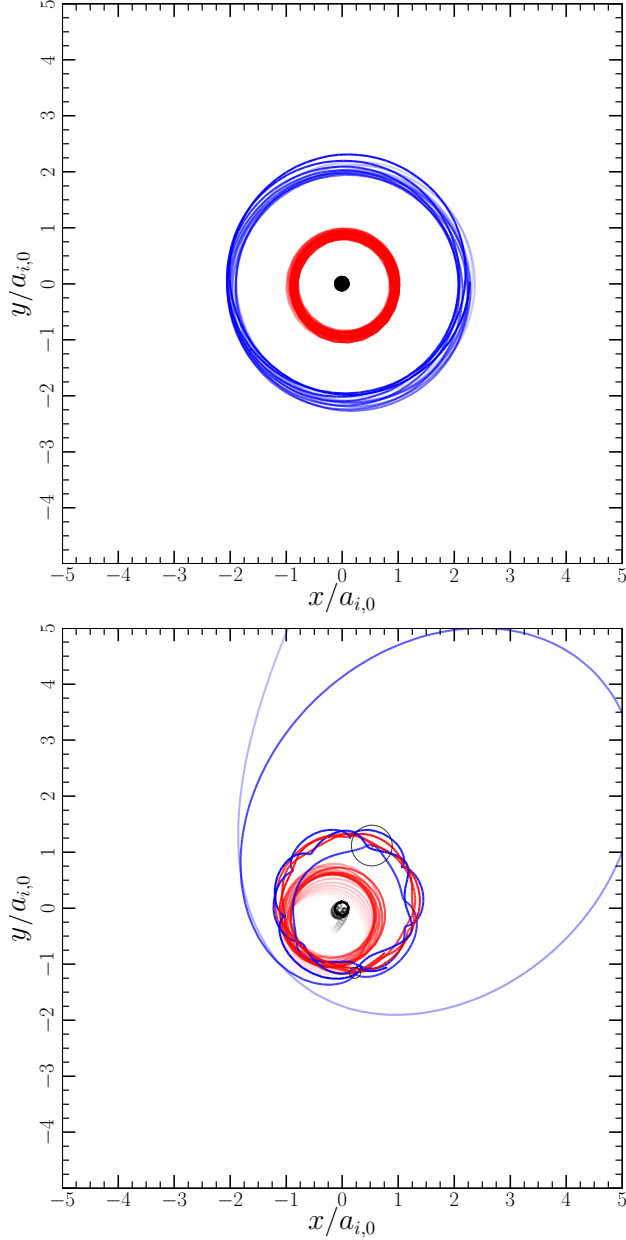$$p(e) \propto \exp(-e/0.05) \,. \quad (4)$$

FIG. 5.— Evolution of a planet/brown dwarf binary system from model t21 resulting in a somewhat gradual tidal capture. Conventions are as in Fig. 3. A weak tidal encounter (the smaller of the two open circles) nearly results in a dynamically stable planet–planet binary. The planets later suffer a stronger tidal encounter (the larger of the two open circles) that results in a stable configuration. Note that the radius of the open circles is proportional to the fractional change in relative planet–planet velocity resulting from the encounter. In this case, the planet–planet binary's circularized semi-major axis is $6.0\,R_\odot$.

We require for each binary pair, chosen according to the above prescriptions, that its orbital separation $a_{\rm circ}$ be smaller than 40% of the radius of the Hill sphere for that particular binary (this depends on the masses and the eccentricity of the outer binary) in order to ensure long-term stability (Domingos et al. 2006).[10] Once the

[10] Their stability criteria apply to the case of massless satellites of planets. We have performed some numerical tests for equal-mass planet–planet binaries in circular orbits and obtained similar
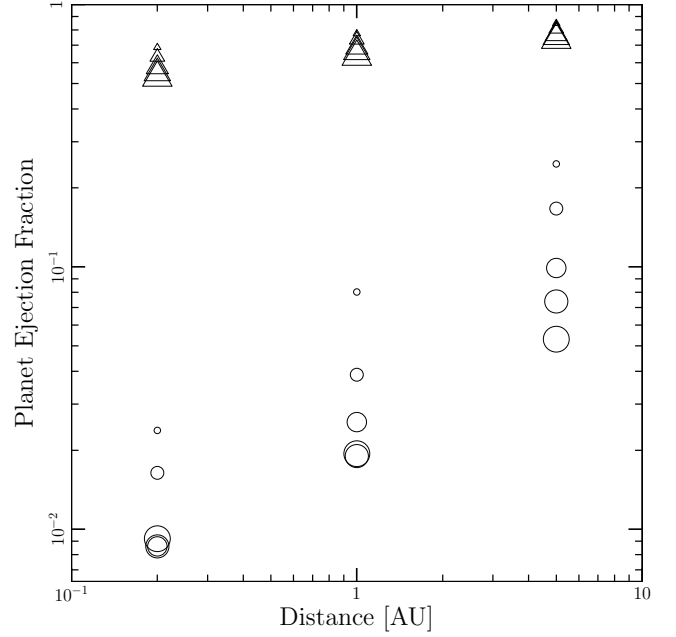

FIG. 6.— The fraction of dynamically active planet systems in which one of the planets is ejected as a function of the distance from the parent star. Triangles are for "planets" in the brown-dwarf mass range, while circles represent gas giants of approximately Jupiter's mass. Symbol size is proportional to the log of the planet/brown dwarf radius.

FIG. 7.— The fraction of dynamically active planet systems in which a successful tidal capture occurs leading to the formation of a stable binary planet. Triangles are for "planets" in the brown-dwarf mass range, while circles represent gas giants of approximately Jupiter's mass. Symbol size is proportional to the log of the planet/brown dwarf radius.
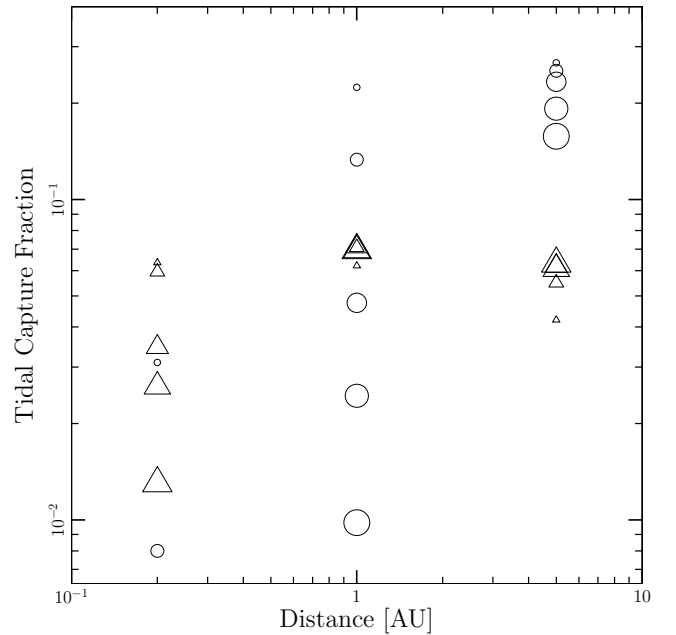
parameters of a binary have been fully chosen, we assign a probability of detection via transits simply as $\propto R_*/d$,

stability boundaries.

The results of our simulations are shown in Fig. 8 for three different mass pairs of planets/brown dwarfs. The top, middle, and bottom panels are for the mass pairs: $\{70, 30\}, \{20, 10\}, \{1, \frac{1}{2}\}$ Jupiter masses, respectively. In each panel the color shading is proportional to the relative probability of finding a transiting binary pair at planet distance, d, and planet separation, a_{circ}. The radius of the Hill sphere is shown as the diagonal green line.

3. DETECTABILITY OF A PLANET–PLANET BINARY
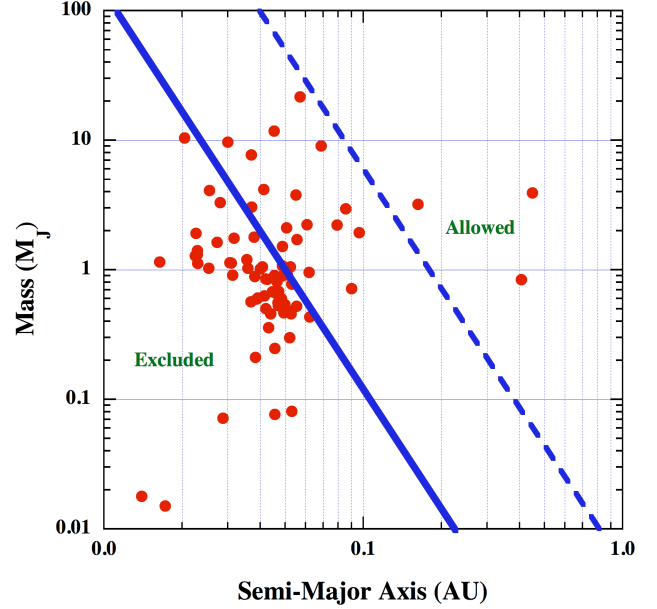
FIG. 9.— The ~ 80 known transiting exoplanet systems (taken from "The Extrasolar Encyclopedia" [http://exoplanet.eu/catalog-all]) in the planet mass–semimajor axis plane. The blue line divides the allowed from excluded region of this space if the binary planet must fit within 40% of its Hill sphere and the binary components are separated by at least 3 R_{J}. The dashed line is slightly more conservative (see text).

In this work we have shown that if planets are dynamically active early in their history, and that our prescription for tidal interactions is plausibly accurate, then binary planets should form with comparable frequency with which others are ejected. Therefore, since dynamically active planets are the currently favored mechanism for the formation of eccentric exoplanet orbits (Ford & Rasio 2008; Jurić & Tremaine 2008; Chatterjee et al. 2008), we expect that there exist gas-giant binary planets among the ~ 420 that are currently known. In this section we discuss the signatures that such hypothetical binary planets would exhibit in observations of the currently known sample of exoplanets, and prospects for detecting them in future studies.

Since most of the known exoplanets have been discovered via radial velocity (hereafter, "RV") measurements, the first question to answer is how large would be the perturbations to the observed Doppler signature. Treating the binary planet as an orbital perturbation, we derived an expression for the maximum deviations from a conventional RV curve of the central star due to the influence
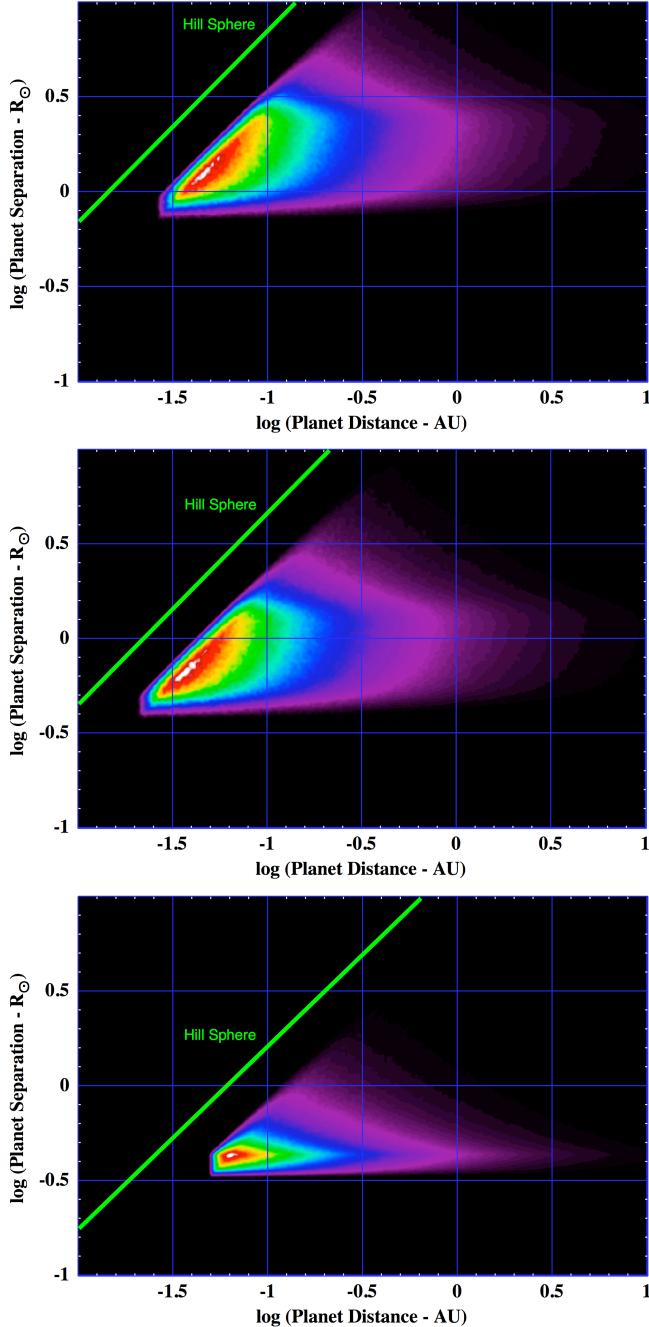

FIG. 8.— Simulated populations of Jovian binary planets (bottom panel), super-Jupiter binary planets (middle panel) and binary brown dwarfs (top panel) in orbit about the parent star (in this case, $1\,M_{\odot}$). The masses of each binary pair are $\{70, 30\}, \{20, 10\}, \{1, \frac{1}{2}\}$ Jupiter masses (top to bottom panels). The color shading indicates the relative probability of discovering such a system, assuming that the binaries are born uniformly distributed in $\log d$. White to purple colors indicate probability ratios of $\sim 50 : 1$. See text for specific algorithms used here. The radius of the Hill sphere is indicated by the diagonal green line.

where d is the distance of the binary CM from the parent star of radius R_{*}. Obviously, this probability could be enhanced if the projected separation of the planet/brown-dwarf binary, as seen from the Earth, is larger than the parent star. However, such calculations are beyond the scope of the paper.

TABLE 1
PARAMETERS FOR PLANET EVOLUTION SIMULATIONS.

model name	$m_1/10^{-3}\,M_\odot$	$m_2/10^{-3}\,M_\odot$	$R_1/R_\odot$	$R_2/R_\odot$	$a_{1,\text{init}}/\text{AU}$	tidal dissipation
t2	1	1	0.1	0.1	5	off
t3	3	3	0.1	0.1	5	off
t4	4	2	0.1	0.1	5	off
t5	4	2	0.1	0.1	5	on
t6	50	25	0.1	0.1	5	on
t7	4	2	0.1	0.1	0.2	on
t8	50	25	0.1	0.1	0.2	on
t9	1	0.5	0.1	0.1	5	on
t10	70	30	0.1	0.1	5	on
t11	1	0.5	0.1	0.1	1	on
t12	70	30	0.1	0.1	1	on
t13	1	0.5	0.1	0.1	0.2	on
t14	70	30	0.1	0.1	0.2	on
t15	70	30	0.2	0.2	0.2	on
t16	1	0.5	0.2	0.2	5	on
t17	70	30	0.2	0.2	5	on
t18	1	0.5	0.2	0.2	1	on
t19	70	30	0.2	0.2	1	on
t20	1	0.5	0.2	0.2	0.2	on
t21	70	30	0.6	0.4	0.2	on
t22	1	0.5	0.4	0.4	5	on
t23	70	30	0.4	0.4	5	on
t24	1	0.5	0.4	0.4	1	on
t25	70	30	0.4	0.4	1	on
t26	1	0.5	0.4	0.4	0.2	on
t27	70	30	0.4	0.4	0.2	on
t28	1	0.5	0.6	0.6	5	on
t29	70	30	0.6	0.6	5	on
t30	1	0.5	0.6	0.6	1	on
t31	70	30	0.6	0.6	1	on
t32	1	0.5	0.6	0.6	0.2	on
t33	70	30	0.6	0.6	0.2	on
t34	1	0.5	0.8	0.8	5	on
t35	70	30	0.8	0.8	5	on
t36	1	0.5	0.8	0.8	1	on
t37	70	30	0.8	0.8	1	on
t38	1	0.5	0.8	0.8	0.2	on
t39	70	30	0.8	0.8	0.2	on
t40	1	0.5	0.2	0.2	0.04	on

NOTE. — The quantities m_i and R_i are the planet masses and radii, and $a_{1,\text{init}}$ is the initial semi-major axis of planet 1. At least 5000 simulations were run for each model.

of a binary planet as

$$\Delta V_r \simeq \frac{9}{32} \left(\frac{a}{R_0} \right)^2 \left(\frac{\Omega_0}{\omega} \right) \left(\frac{2m}{M} \right) V_0\,, \qquad (5)$$

where a is the orbital separation of the binary planets, R_0 and Ω_0 are the mean orbital radius of the outer binary and its mean angular velocity, respectively, $V_0 = \Omega_0 R_0$, ω is the synodic orbital period of the binary planet, m is the mass of an assumed equal-mass member of the binary planet, and M is the mass of the parent star. The mean orbits of the inner and outer binaries have been taken as circular and coplanar for simplicity. Since the ratio Ω_0/ω can be expressed in terms of the masses and orbital radii involved, we can write

$$\Delta V_r \simeq \frac{9}{32} \left(\frac{a}{R_0} \right)^{7/2} \sqrt{\frac{2m}{M}}\, V_0\,. \qquad (6)$$

For a binary planet with an orbital separation of $a = 0.4\,R_{\text{Hill}} \simeq 0.4\,(2m/3M)^{1/3}$, i.e., the largest stable separation, we have

$$\Delta V_r^{\max} \simeq \frac{9}{32} \left(\frac{8}{375} \right)^{7/6} \left(\frac{2m}{M} \right)^{5/3} V_0\,. \qquad (7)$$

For illustrative values of $m = M_{\text{J}}$ and $V_0 = 30$ km s^{-1}, the numerical value of $\Delta V_r^{\max}$ is $\sim 0.3\,\text{cm s}^{-1}$, far too small to be detected in current observations as well as those that are currently planned for the near future. On the other hand, for a binary brown dwarf of, e.g., $50\,M_{\text{J}}$, the expected perturbations to the RV curve would be of order 2 m s^{-1}, which would be detectable. Thus, it seems fair to say that the existence of gas-giant planets would not have been noticed in exoplanet RV curves.

We next consider whether binary planets would have been detected among any of the ~ 80 currently known transiting exoplanets. For these systems, the transit light curves would be manifestly anomalous and the presence of two planets would be quite obvious. In Fig. 9 we show a plot of 80 currently known transiting exoplanets in the planet mass–semimajor axis plane. Note that, as expected, most of these systems are close to the parent star (i.e., $\lesssim 0.1$ AU), thereby enhancing their transit probability. The solid blue line indicates where in this plane a binary planet can fit within 40% of its Hill sphere and still allow the binary to be separated by at least 3 times the radius of Jupiter, thereby avoiding Roche lobe overflow from one planet to another. In this conservative set of restrictions, we see that only $\sim 1/4$ of the systems could

TABLE 2
OUTCOME NUMBERS FOR PLANET EVOLUTION SIMULATIONS.

model name	total	ejection	collision	tidal capture	two planets	stargrazer	error[a]
t2	5000	1450	2359	0	1124	6	61
t3	5000	2386	1777	0	830	5	2
t4	5000	2436	1628	0	805	123	8
t5	5000	1969	1377	969	642	33	10
t6	5000	3934	373	272	395	25	1
t7	5000	335	3804	286	550	25	0
t8	5000	2760	1426	376	303	127	8
t9	5000	1234	2112	1337	309	1	7
t10	5000	4275	301	212	165	47	0
t11	5000	401	3348	1121	127	0	3
t12	5000	3905	612	313	106	64	0
t13	5000	119	4653	155	71	1	1
t14	5000	3461	1030	320	41	148	0
t15	5000	3213	1334	302	31	119	1
t16	5000	834	2685	1262	214	1	4
t17	5000	4112	428	279	144	37	0
t18	5000	194	4042	666	97	0	1
t19	5000	3734	771	360	78	57	0
t20	5000	82	4809	40	67	2	0
t21	100000	58772	36438	2389	532	1856	13
t22	5000	495	3204	1166	133	0	2
t23	5000	3957	571	317	118	37	0
t24	5000	128	4556	238	76	0	2
t25	5000	3517	1001	365	55	62	0
t26	5000	43	4892	4	61	0	0
t27	5000	2959	1743	177	27	94	0
t28	5000	369	3548	961	120	0	2
t29	5000	3885	657	312	104	41	1
t30	5000	95	4715	122	67	0	1
t31	5000	3404	1132	357	47	60	0
t32	5000	43	4897	3	57	0	0
t33	5000	2828	1928	134	27	82	1
t34	5000	265	3851	788	94	1	1
t35	5000	3801	746	325	97	30	1
t36	5000	97	4791	49	62	1	0
t37	5000	3277	1256	358	43	63	3
t38	5000	46	4898	1	54	1	0
t39	5000	2727	2097	67	27	82	0
t40	5000	37	4902	0	60	1	0

NOTE. — We label the outcomes as in Ford & Rasio (2008). "Two planets" refers to a system that has not achieved another outcome (collision, ejection, etc.) within the maximum integration time of 5×10^6 code units ($\sim 8 \times 10^5$ initial orbital periods of planet 1).

[a] For reference, we give the outcome statistics for each model. The final column includes both errors and uncounted outcomes. A typical error is the system becoming dynamically stable (and classified as such) due to integrator energy drift. A typical uncounted outcome is one planet being ejected while the other collides with the host star.

possibly harbor a binary planet. If we make these constraints only somewhat more 'comfortable' by requiring that the planets be separated by at least 5 $R_{\rm J}$ and that this separation be less than 1/5 of the radius of the Hill sphere, the separatrix is shown with a dashed blue line. In that case, it seems quite plausible that no more than three of the currently known transiting systems could contain a binary planet. At the moment, the numerical simulations presented in this work do not place tight constraints on the ratio of highly eccentric exoplanet orbits and those with binary planets, nor can they predict an absolute fraction of exoplanets that should be binary. Nonetheless, it is by no means obvious that any binary planets should have yet been detected by either RV or transit light curve studies.

It is also possible that binary planets could be detected with gravitational lensing. The Einstein radius, $R_{\rm E}$, of a single planet of mass, m, at a distance D, and a generic source at $\sim 2D$, projected back to the lens plane has a physical size

$$R_{\rm E} \simeq \sqrt{\frac{2GMD}{c^2}} \simeq 0.06\,{\rm AU}\sqrt{\frac{mD_{\rm kpc}}{M_{\rm J}}} \ . \qquad (8)$$

Thus, if the planet is actually a binary, it would have to have an orbital separation comparable to, or greater than $R_{\rm E}$, in order for its binary nature to be readily revealed in the microlensing light curves. For comparison, the maximum separation between binary components of a Jupiter mass at an AU from a 1 $M_\odot$ star is ~ 0.03 AU.

Probably the best hope for detecting binary planets is to obtain a larger sample of transiting exoplanets, yielding a substantial number (e.g., $\gtrsim$ a dozen) at distances from the parent star of $\gtrsim 0.4$ AU. The Kepler mission should ultimately provide such a sample. At these larger distances for transiting exoplanets, there is more phase space to fit stable binaries within their Hill sphere and to allow larger separations between the binary components.
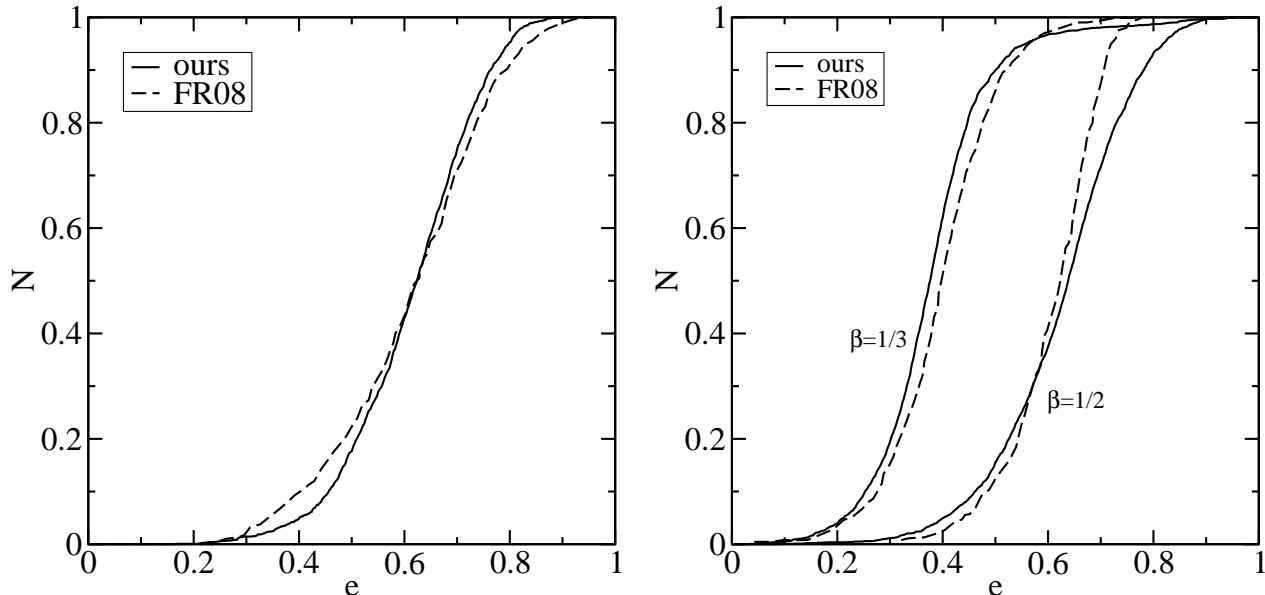
FIG. 10.— *Left Panel:* Comparison with Fig. 2 of Ford & Rasio (2008), the cumulative eccentricity distribution of the remaining planet after a planet is ejected for the case $m_1/M_\star = m_2/M_\star = 10^{-3}$. As in Ford & Rasio (2008), we set the stellar mass to $M_\star = 1\,M_\odot$ and the planet masses to $m_i = 10^{-3}\,M_\odot$. *Right Panel:* Comparison with Fig. 3 of Ford & Rasio (2008), the cumulative eccentricity distribution of the remaining planet after a planet is ejected for $\beta \equiv m_1/m_2 = 1/2$ and $\beta = 1/3$. As in Ford & Rasio (2008), we set $m_1 + m_2 = 6 \times 10^{-3} M_\star$ and $M_\star = 1\,M_\odot$.

If gas-giant binary planets are ultimately discovered, they would represent a strong corroboration of the dynamically active scenario, since gas giant binaries formed via tidal capture are a natural outcome of dynamically active systems. On the other hand, if no binary planets are detected, even with a larger sample of transiting exoplanets, it may simply be that our treatment of the tidal capture process is too optimistic. Parameters of the tidal capture process could be constrained by comparing N-body simulations that allow for tidal capture with observed planet eccentricity distributions, with the restriction that no observable planet–planet binaries be formed.

APPENDIX

USE OF THE FEWBODY DYNAMICAL CODE

In our numerical simulations we use the *Fewbody* integrator, which is designed for strong small-N-body gravitational encounters (Fregeau et al. 2004). To test *Fewbody*'s suitability for dynamically active planetary systems, we compare our scattering calculations with the work of Ford & Rasio (2008), who studied planet–planet scattering with the aim of explaining the high eccentricities of some observed extrasolar planetary systems. As with most studies of planet–planet scattering, they used a mixed variable symplectic method modified to treat close encounters (Wisdom & Holman 1991; Chambers 1999). When this method is applied to a two-planet system, a close encounter between the planets results in *all* orbital motion being integrated with a standard, non-symplectic integrator (e.g., Bulirsch-Stoer). Since the two-planet systems we study are dynamically active and hence quickly result in close approaches, their evolution should be faithfully treated (in a statistical sense) with the adaptive, but non-symplectic, integration algorithm in *Fewbody*.

Fig. 10 (left panel) shows a comparison of our numerical method with Fig. 2 of Ford & Rasio (2008), who integrated the evolution of dynamically active two-planet systems. Specifically, the cumulative eccentricity distribution of the remaining planet after a planet is ejected is shown for the case $m_1/M_\star = m_2/M_\star = 10^{-3}$, where m_i is the mass of planet i and $M_\star$ is the mass of the host star. By convention, planet 1 initially orbits with semi-major axis $a_{1,\mathrm{init}} < a_{2,\mathrm{init}}$. Our initial conditions (including planet eccentricities, relative inclinations, and randomization of various orbital elements) are the same as in Ford & Rasio (2008). Most notably for this case, we similarly set the stellar mass to $M_\star = 1\,M_\odot$ and the planet masses to $m_i = 10^{-3}\,M_\odot$. As is clear from the figure, the eccentricity distributions are fairly similar – in fact, the median eccentricity is the same in both distributions. The differences are most apparent at low and high eccentricities. Part of the discrepancy may arise from our differing definitions of ejection. In Ford & Rasio (2008), a planet straying beyond $2000a_{1,\mathrm{init}}$ is declared to have been ejected, while in *Fewbody* a planet is not considered ejected until it is formally unbound from and receding from the remaining masses, and is sufficiently weakly tidally coupled to the remaining masses that it could never become bound again. Another source for the discrepancy may be the accuracy of the mixed variable symplectic method for close star–planet approaches used in Ford & Rasio (2008). As pointed out in Rauch & Holman (1999), the method introduces artificial chaos for close star–planet approaches. Finally, a remaining source for the discrepancy may be the calculation stopping time. We used a stopping time of

5×10^6 code units ($\sim 8 \times 10^5$ initial orbital periods of planet 1) for all calculations. Ford & Rasio (2008) used a stopping time between 5×10^6 and 2×10^7 that is an unspecified function of the planet masses.

Fig. 10 (right panel) shows a comparison of our results with Fig. 3 of Ford & Rasio (2008). Shown is the cumulative eccentricity distribution of the remaining planet after a planet is ejected for $\beta \equiv m_1/m_2 = 1/2$ and $\beta = 1/3$. As in Ford & Rasio (2008), we set $M_\star = 1\,M_\odot$ and $m_1 + m_2 = 6 \times 10^{-3}M_\star$ to speed up the evolution. (As shown in Ford & Rasio (2008), the final eccentricity distribution is not sensitive to the ratio $(m_1 + m_2)/M_\star$ for $m_i/M_\star \sim 10^{-3}$, but the time to ejection decreases as $(m_1 + m_2)/M_\star$ increases.) While the agreement between the eccentricity distributions is not perfect, our results agree fairly well with those of Ford & Rasio (2008), and reproduce the dependence of the eccentricity distribution on β. Additionally, eccentricities above 0.8 are very rare, as found in Ford & Rasio (2008).

REFERENCES

Auvergne, M., Bodin, P., Boisnard, L., Buey, J., Chaintreuil, S., & others. 2009, A&A, 506, 411
Basri, G., Borucki, W. J., & Koch, D. 2005, NewAR, 49, 478
Bodenheimer, P., Lin, D. N. C., & Mardling, R. A. 2001, ApJ, 548, 466
Boss, A. P. 1997, Science, 276, 1836
Bouchy, F., Deleuil, M., Guillot, T., Agrain, S., & others. 2010, submitted
Canup, R. M. & Asphaug, E. 2001, Nature, 412, 708
Carter, J. A. & Winn, J. N. 2010, ApJ, 716, 850
Chambers, J. E. 1999, MNRAS, 304, 793
Chatterjee, S., Ford, E. B., Matsumura, S., & Rasio, F. A. 2008, ApJ, 686, 580
Domingos, R. C., Winter, O. C., & Yokoyama, T. 2006, MNRAS, 373, 1227
Fabian, A. C., Pringle, J. E., & Rees, M. J. 1975, MNRAS, 172, 15P
Ford, E. B. & Rasio, F. A. 2008, ApJ, 686, 621
Fregeau, J. M., Cheung, P., Portegies Zwart, S. F., & Rasio, F. A. 2004, MNRAS, 352, 1
Gladman, B. 1993, Icarus, 106, 247

Goldreich, P., Lithwick, Y., & Sari, R. 2002, Nature, 420, 643
Goldreich, P. & Soter, S. 1966, Icarus, 5, 375
Hartmann, W. K. & Davis, D. R. 1975, Icarus, 24, 504
Jurić, M. & Tremaine, S. 2008, ApJ, 686, 603
Lee, M. H. & Peale, S. J. 2002, ApJ, 567, 596
Lin, D. N. C. 1981, MNRAS, 197, 1081
Mardling, R. A. 1995, ApJ, 450, 732
Mardling, R. A. 2008, in Lecture Notes in Physics, Berlin Springer Verlag, Vol. 760, The Cambridge N-Body Lectures, ed. S. J. Aarseth, C. A. Tout, & R. A. Mardling, 59–+
Matsumura, S., Thommes, E. W., Chatterjee, S., & Rasio, F. A. 2010, ApJ, 714, 194
Nelson, L. A., Rappaport, S., & Joss, P. C. 1993, ApJ, 404, 723
Papaloizou, J. C. B. & Szuszkiewicz, E. 2005, MNRAS, 363, 153
Portegies Zwart, S. F. & Meinen, A. T. 1993, A&A, 280, 174
Rauch, K. P. & Holman, M. 1999, AJ, 117, 1087
Stamatellos, D. & Whitworth, A. P. 2009, MNRAS, 392, 413
Thommes, E. W., Matsumura, S., & Rasio, F. A. 2008, Science, 321, 814
Toomre, A. 1964, ApJ, 139, 1217
Wisdom, J. & Holman, M. 1991, AJ, 102, 1528